

# Photodisintegration cross section of deuteron

M.Odsuren<sup>1\*</sup>, A.T.Sarsembayeva<sup>2</sup>, G.Khuukhenkhuu<sup>1</sup>, S.Davaa<sup>1</sup>, K.Katō<sup>3</sup>

<sup>1</sup> School of Engineering and Applied Sciences and Nuclear Research Center, National University of Mongolia, Ulaanbaatar 210646, Mongolia

<sup>2</sup> Al-Farabi Kazakh National University, Almaty 050040, Kazakhstan

<sup>3</sup> Nuclear Reaction Data Centre, Faculty of Science, Hokkaido University, Sapporo 060-0810, Japan

The peak produced by the M1 and E1 transition strengths for the photodisintegration cross section of deuteron is calculated in the complex scaling method and the origin of the peak of the M1 strength near threshold energy is discussed.

Keywords: Few-body model, photo-disintegration cross section, virtual state.

## INTRODUCTION

A virtual-state character on light nuclei including halo nuclei has been studied using different theoretical methods, namely, the analytical continuation method [1] and the Jost function method [2] and the microscopic cluster model [3].

A virtual state plays an important role in reaction cross sections just above the breakup threshold energy, such as producing the peak behavior. However, the virtual state cannot be directly obtained as an isolated pole solution in the complex scaling method (CSM) [4-5] because of a limit of the scaling angle in the CSM. In 2017, we proposed a useful approach to find the pole position of the virtual state calculating the continuum level density (CLD), the scattering phase shift, and scattering length calculated in the CSM [6].

In the next step, we applied the CSM to the two-body  ${}^8\text{Be}+n$  model and we observed the photodisintegration cross section for the  $1/2^+$  state in  ${}^9\text{Be}$  has a peculiar enhancement near the  ${}^8\text{Be}+n$  threshold energy. The origin of the peak is investigated in relation to the virtual state of  ${}^9\text{Be}$  in the CSM. We showed that the real part of the matrix element and the imaginary part of the level density are dominant for the contributions of the components of the  $E1$  strength function [7].

The purpose of this work is to calculate the photodisintegration cross section just above the threshold energy of the virtual state using a neutron-proton model which simulates the deuteron. Experiments on the scattering of neutrons by *ortho* and *para*-hydrogen have led to the conclusion that the  ${}^1S_0$  state is a virtual state having a negative

binding energy [8]. We investigate the  $M1$  transition strength of the photodisintegration cross section of neutron-proton system.

## THEORETICAL FRAMEWORK

**Two-body model in the complex scaling method**  
We solve the Schrödinger equation applying the CSM

$$\hat{H}^\theta \Psi_{J^\pi}^v(\theta) = E_v^\theta \Psi_{J^\pi}^v(\theta) \quad (1)$$

where,  $J$  is the total spin and  $v$  is the state index. The complex-scaled Hamiltonian and wave function are given as  $\hat{H}^\theta = U(\theta)\hat{H}U(\theta)^{-1}$  and  $\Psi_{J^\pi}^v(\theta) = U(\theta)\Psi_{J^\pi}^v$ , respectively (see Refs. [5, 9] for detail). The complex scaling operator  $U(\theta)$  transforms the relative coordinate  $r$  as

$$U(\theta): r \rightarrow r \exp(i\theta) \quad (2)$$

where,  $\theta$  is the scaling angle being a positive real number.

Hamiltonian  $\hat{H}$  consists of the relative kinetic energy  $T = -\frac{\hbar^2}{2\mu}\nabla_r^2$ , where  $\mu$  is the reduced mass, and potential  $V(r)$  for relative motion:

$$\hat{H} = -\frac{\hbar^2}{2\mu}\nabla_r^2 + V(r) \quad (3)$$

As  $L^2$ -basis functions, we employ Gaussian basis functions, and then the radial wave function is expressed as

$$\Psi_\ell^v(\theta) = \sum_{n=1}^N c_n^{\ell,v}(\theta) \phi_n^\ell(r) \quad (4)$$

where,  $\{\phi_n^\ell(r)\}$  is the Gaussian basis function set. The expansion coefficients  $c_n^{\ell,v}(\theta)$  and the complex

\*Electronic address: odsurenn@gmail.com

energy eigenvalues  $E_\nu^\theta$  are obtained by solving the complex scaled eigenvalue problem given in Eq. (1).

### Photodisintegration cross section

Using the complex-scaled Green's function, we calculate the cross section of the photodisintegration of  $\gamma D \rightarrow n + p$  in terms of the electromagnetic multipole responses. In the present calculation, we focus on the low-lying region of the photodisintegration cross section and take into account the electromagnetic dipole responses.

The photodisintegration cross section  $\sigma^\nu$  is given by the sum of those by the  $E1$  and  $M1$  transitions as

$$\sigma^\nu(E_\gamma) = \sigma_{E1}(E_\gamma) + \sigma_{M1}(E_\gamma), \quad (5)$$

where,  $E_\gamma$  is the incident energy of photon.

The cross sections for the electromagnetic dipole transitions  $\sigma_{EM1}$  are expressed as the following form:

$$\sigma_{EM1}(E_\gamma) = \frac{16\pi^3}{9} \left( \frac{E_\gamma}{\hbar c} \right)^2 \frac{dB(EM1, E_\gamma)}{dE_\gamma}. \quad (6)$$

Using the CSM and the complex-scaled Green's function, the electromagnetic dipole transition strength is calculated as

$$\begin{aligned} \frac{dB(EM1, E_\gamma)}{dE_\gamma} &= -\frac{1}{\pi} \frac{1}{2J+1} \\ &\times \text{Im} \left[ \sum_\nu^N \langle \tilde{\Psi}_j(\theta) | (\hat{O}^\theta)^\dagger (EM1) | \Psi_j^\nu(\theta) \rangle \right. \\ &\times \left. \frac{1}{E-E_\nu^\theta} \langle \tilde{\Psi}_j^\nu(\theta) | \hat{O}^\theta (EM1) | \Psi_j(\theta) \rangle \right] \quad (7) \end{aligned}$$

where  $J$  represents the total spin.  $E = E_\gamma - E_{th}$  and  $E_{th} = 2.23$  MeV is the deuteron binding energy, and  $\hat{O}^\theta(EM1)$  is an electromagnetic dipole transition operator.

### Continuum Level Density

We can write Eq. (7) as

$$\frac{dB(EM1, E_\gamma)}{dE_\gamma} = \frac{1}{2J+1} \text{Im} \sum_\nu \{ M_\nu^2 \rho_\nu(E) \} \quad (8)$$

where matrix element  $M_\nu^2$

$$\begin{aligned} M_\nu^2 &= \langle \tilde{\Psi}_{J_{gs}}^{gs}(\theta) | (\hat{O})^\dagger (EM1) | \Psi_j^\nu(\theta) \rangle \\ &\times \langle \tilde{\Psi}_j^\nu(\theta) | \hat{O}(EM1) | \Psi_{J_{gs}}^{gs}(\theta) \rangle \quad (9) \end{aligned}$$

and level density  $\rho_\nu(E)$

$$\rho_\nu(E) = -\frac{1}{\pi} \frac{1}{E-E_\nu^\theta} \quad (10)$$

It is noted that  $M_\nu^2$  and  $\rho_\nu$  are complex numbers and do not directly correspond to physical quantities.

The level density of states  $\rho_\theta^N(E)$  for the basis number  $N$  is expressed as

$$\begin{aligned} \rho_\theta^N(E) &= \sum_{B=1}^{N_B} \delta(E - E_B) - \frac{1}{\pi} \text{Im} \sum_{R=1}^{N_R^\theta} \frac{1}{E-E_R} \\ &- \frac{1}{\pi} \text{Im} \sum_{k=1}^{N-N_B-N_R^\theta} \frac{1}{E-\varepsilon_k(\theta)} \quad (11) \end{aligned}$$

The complex energies of resonant states are obtained as  $E_r = E_r^{res} - i\Gamma_r/2$ , when  $\tan^{-1}(\Gamma_r/2E_r^{res}) < 2\theta$  and thus each resonance term has the Breit-Wigner form

$$\text{Im} \frac{1}{E-E_R} = \frac{-\Gamma_r/2}{(E-E_R)^2 + \Gamma_r^2/4} \quad (12)$$

For the continuum part, discretized continuum states are obtained on the  $2\theta$  line in the complex energy plane,  $\varepsilon_k(\theta) = \varepsilon_k^{Re} - i\varepsilon_k^{Im}$ , where  $\frac{\varepsilon_k^{Im}}{\varepsilon_k^{Re}} = \tan 2\theta$ .

Therefore, the continuum term in the level density can be expressed in terms of a Lorentzian function whose form is similar to the Breit-Wigner form:

$$\text{Im} \frac{1}{E-\varepsilon_k(\theta)} = \frac{-\varepsilon_k^{Im}}{(E-\varepsilon_k^{Re})^2 + \varepsilon_k^{Im^2}} \quad (13)$$

Using the Breit-Wigner form and a Lorentzian function, we can write the level density in the basis function method as

$$\begin{aligned} \rho_\theta^N(E) &= \sum_{B=1}^{N_B} \delta(E - E_B) \\ &+ \frac{1}{\pi} \text{Im} \sum_{R=1}^{N_R^\theta} \frac{\Gamma_r/2}{(E-E_R)^2 + \Gamma_r^2/4} \\ &+ \frac{1}{\pi} \text{Im} \sum_{k=1}^{N-N_B-N_R^\theta} \frac{\varepsilon_k^{Im}}{(E-\varepsilon_k^{Re})^2 + \varepsilon_k^{Im^2}} \quad (14) \end{aligned}$$

Solving the eigenvalue problem, we obtain energies  $E_\nu^\theta$  and wave functions  $\Psi_j^\nu(\theta)$  for  $\nu = 1, 2, \dots, N$ . The energies of complex numbers in the CSM are generally classified to three groups; bound state energies ( $E_B$ : real and  $< 0$ ), resonant state energies ( $E_R$ ) and continuum state energies ( $\varepsilon_k(\theta)$ ). Here, it is worthwhile to note that  $E_B$  and  $E_R$  are independent from  $\theta$  while  $\theta$ -dependent  $\varepsilon_k(\theta)$  are obtained along the  $2\theta$  line in the complex energy plane. Using the energy solutions ( $E_\nu^\theta, E_{0\nu}^\theta$ ) of the Hamiltonian  $\hat{H}^\theta$  and the free-Hamiltonian  $\hat{H}_0^\theta$

without potential terms, we can construct the continuum level density (CLD)  $\Delta E$  [10-12]

$$\Delta E = \rho_{\theta}^N(E) - \rho_{0(\theta)}^N(E) \quad (15)$$

## RESULTS AND DISCUSSIONS

### Deuteron photodisintegration cross section

We approximate the ground state of deuteron by the  $^3S_1$  configuration and the virtual state is described by the  $^1S_0$  state. For the potential we use the Hasegawa-Nagata (HN) force (No.2) [13-14] which is expressed by the three-range Gaussian form. The ground state of deuteron can be expressed by a dominant configuration of the triplet- $S$  wave ( $^3S_1$ ) when the tensor force is neglected. The tensor force brings a coupled channel equation of  $^3S_1+^3D_1$ , and its result indicates a  $\sim 4\%$  mixing of the  $^3D_1$  configuration.

For the final state of the magnetic dipole transition, we consider  $^1S_0$  state. Therefore, we solve Eq. (1) for the ground state of deuteron using the following neutron-proton potential of the HN No.2 for the  $^3S_1$  state in Eq.(3)

$$V_{3S}(r) = -V_0 \exp(-\alpha r^2) - V_1 \exp(-\beta r^2) + V_2 \exp(-\gamma r^2) \quad (16)$$

and for the final ( $^1S_0$  virtual) state

$$V_{1S}(r) = -V_0 \exp(-\alpha r^2) - V_1 \exp(-\beta r^2) + V_2 \exp(-\gamma r^2) \quad (17)$$

Table 1 Potential parameters of the  $^3S_1$  and  $^1S_0$  states.

Potential parameters, units	$^3S_1$ ground state	$^1S_0$ virtual state
$V_0$ [MeV]	6.0	5.0
$V_1$ [MeV]	546.0	360.0
$V_2$ [MeV]	1655.0	1144.6
$\alpha$ [fm $^{-2}$ ]	0.16	0.16
$\beta$ [fm $^{-2}$ ]	1.127	1.127
$\gamma$ [fm $^{-2}$ ]	3.4	3.4

Near the threshold with  $E_{\gamma} \leq 10$  MeV, the deuteron photodisintegration  $\gamma + D \rightarrow n + p$  is dominated by the  $M1$  transition  $D \rightarrow ^1S_0$  and the  $E1$  transition  $D \rightarrow ^3S_1$ .

These  $M1$  and  $E1$  transition strengths are

$$\begin{aligned} \frac{dB(M1, E_{\gamma})}{dE_{\gamma}} &= -\frac{1}{\pi} \frac{1}{2J+1} \\ &\times \text{Im} \left[ \sum_{\nu}^N \langle \tilde{\Psi}_{\nu}(\theta) | (\hat{O}^{\theta})^+ (M1) | \Psi_{\nu}^{\gamma}(\theta) \rangle \right. \\ &\quad \left. \times \frac{1}{E-E_{\nu}^{\theta}} \langle \tilde{\Psi}_{\nu}^{\gamma}(\theta) | \hat{O}^{\theta} (M1) | \Psi_{\nu}(\theta) \rangle \right] \end{aligned} \quad (17)$$

and

$$\begin{aligned} \frac{dB(E1, E_{\gamma})}{dE_{\gamma}} &= -\frac{1}{\pi} \frac{1}{2J+1} \\ &\times \text{Im} \left[ \sum_{\nu}^N \langle \tilde{\Psi}_{\nu}(\theta) | (\hat{O}^{\theta})^+ (E1) | \Psi_{\nu}^{\gamma}(\theta) \rangle \right. \\ &\quad \left. \times \frac{1}{E-E_{\nu}^{\theta}} \langle \tilde{\Psi}_{\nu}^{\gamma}(\theta) | \hat{O}^{\theta} (E1) | \Psi_{\nu}(\theta) \rangle \right] \end{aligned} \quad (18)$$

In Fig. 1, the calculated  $\gamma D \rightarrow np$  photodisintegration cross section is shown in comparison with experimental data. The calculated results well reproduce the experimental data of the energy distribution of the cross section as shown in Fig. 1 and the experimental data are taken from Refs. [15-16]. Contributions of the  $M1$  and  $E1$  transition strengths are shown by the solid- and open-curves, respectively. The experimental data on the  $E1$  and  $M1$  are taken from Refs. [15] (open diamonds) and [16] (filled triangles).

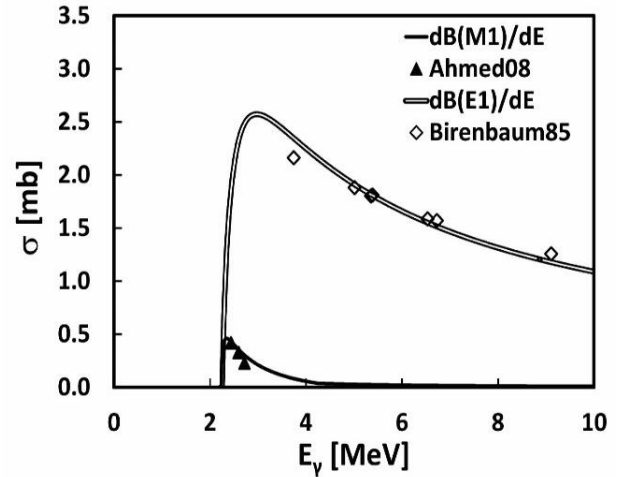


Figure 1. The photodisintegration cross section of deuteron as a function of the energy. Contributions of the  $E1$  and  $M1$  transitions are given by open and solid curves, respectively. The experimental data are taken from Refs. [15] for  $E1$  and [16] for  $M1$ .

We can see a specific energy distribution of the photodisintegration cross section due to the  $M1$  transition calculated with three range Gaussian potential (HN No.2). In our calculation of the two-

body model, there is no parameter to determine the structure of the excited states. However, the calculated photodisintegration cross section, which includes all kinds of contributions of the final states, well explains its observed shape. Therefore, it is very interesting to investigate the origin of the peak form of the cross section.

## CONCLUSION

The  $E1$  and  $M1$  transitions for the photodisintegration cross section of deuteron is calculated by applying three range Gaussian potential (HN No.2). The calculated results agree well with the observed values.

## REFERENCES

- [1] N. Tanaka, Y. Suzuki, K. Varga, R.G. Lovas. Unbound states by analytic continuation in the coupling constant. *Physical Review C* 59, 1391, (1999).
- [2] H. Masui, S. Aoyama, T. Myo, K. Katō, K. Ikeda. Study of virtual states in  $5\text{He}$  and  $10\text{Li}$  with the Jost function method. *Nuclear Physics A* 673, 207-218, (2000)
- [3] P. Descouvemont. Simultaneous study of the  $11\text{Li}$  and  $10\text{Li}$  nuclei in a microscopic cluster model. *Nuclear Physics A* 626, 647-668, (1997).
- [4] Y.K. Ho. The method of complex coordinate rotation and its applications to atomic collision processes. *Physical Reports* 99, 1, (1983).
- [5] S. Aoyama, T. Myo, K. Katō, K. Ikeda. The complex scaling method for many-body resonances and its applications to three-body resonances. *Progress Theoretical Physics* 116, 1, (2006).
- [6] M. Odsuren, Y. Kikuchi, T. Myo, G. Khuukhenkhuu, H. Masui, K. Katō. Virtual-state character of the two-body system in the complex scaling method. *Physical Review C* 95, 064305, (2017).
- [7] M. Odsuren, Y. Kikuchi, T. Myo, H. Masui, K. Katō. Photo-disintegration cross sections for resonant states and virtual states, *Physical Review C* 99, 034312, (2019).
- [8] H.A. Bethe, P. Morrison. *Elementary Nuclear Theory*, second ed., John Wiley & Sons, New York. (1956).
- [9] T. Myo, Y. Kikuchi, H. Masui, K. Katō. Recent development of complex scaling method for many-body resonances and continua in light nuclei. *Progress in Particle and Nuclear Physics* 79, 1, (2014).
- [10] S. Shlomo. Energy level density of nuclei. *Nuclear Physics A* 539, 17-36, (1992).
- [11] R.D. Levine. *Quantum Mechanics of Molecular Rate Processes*. Clarendon Press, Oxford. (1969).
- [12] M. Odsuren, K. Katō, G. Khuukhenkhuu, S. Davaa. Scattering cross section for various potential systems, *Nuclear Engineering and Technology* 49, 1006-1009, (2017).
- [13] A. Hasegawa, S. Nagata, On the behavior of the wave function of the ground state of  ${}^6\text{Li}$ , *Progress Theoretical Physics* 38, 1188-1189, (1967).
- [14] R. Tamagaki. Repulsive core of effective  $\alpha$ - $\alpha$  potential and the Pauli principle. *Supplement of the Progress of Theoretical Physics*, 242-258, (1968).
- [15] Y. Birenbaum, S. Kahane, R. Moreh. Absolute cross section for the photodisintegration of deuterium. *Physics Review C* 32, 1825, (1985).
- [16] M.W. Ahmed, M.A. Blackston, B.A. Perdue, W. Tornow, H.R. Weller, B. Norum, B. Sawatzky, R.M. Prior, M.C. Spraker, Near-threshold deuteron photodisintegration: An indirect determination of the Gerasimov-Drell-Hearn sum rule and forward spin polarizability ( $\gamma_0$ ) for the deuteron at low energies, *Physical Review C* 77, 044005, (2008).